

The structural basis of modularity in ECF-type ABC transporters

Guus B Erkens^{1,2}, Ronnie P-A Berntsson^{1,2}, Faizah Fulyani^{1,2}, Maria Majsnerowska^{1,2}, Andreja Vujičić-Žagar^{1,2}, Josy ter Beek^{1,2}, Bert Poolman^{1,2} & Dirk Jan Slotboom^{1,2}

Energy coupling factor (ECF) transporters are used for the uptake of vitamins in Prokarya. They consist of an integral membrane protein that confers substrate specificity (the S-component) and an energizing module that is related to ATP-binding cassette (ABC) transporters. S-components for different substrates often do not share detectable sequence similarity but interact with the same energizing module. Here we present the crystal structure of the thiamine-specific S-component ThiT from *Lactococcus lactis* at 2.0 Å. Extensive protein-substrate interactions explain its high binding affinity for thiamine ($K_d \sim 10^{-10}$ M). ThiT has a fold similar to that of the riboflavin-specific S-component RibU, with which it shares only 14% sequence identity. Two alanines in a conserved motif (AxxxA) located on the membrane-embedded surface of the S-components mediate the interaction with the energizing module. Based on these findings, we propose a general transport mechanism for ECF transporters.

ABC transporters catalyze the translocation of diverse compounds across membranes and constitute one of the largest superfamilies of proteins¹. They consist of two integral membrane domains that form a translocation pore and two nucleotide-binding domains (NBDs) that drive transport by hydrolyzing ATP. The conserved NBDs are the hallmark of ABC transporters, whereas the transmembrane regions show a large variation in sequence and folds (Fig. 1a). Classical ABC importers require additional extracellular or periplasmic substrate-binding domains or substrate-binding proteins (SBPs) to capture substrates, but the recently discovered ECF transporters use S-components for substrate recognition. S-components associate with an energizing module consisting of the membrane protein EcfT and two identical or homologous NBDs (EcfA and EcfA')².

ECF-type transporters are found in Prokarya only and mediate the uptake of vitamins and other nutrients needed in trace amounts (such as Ni²⁺ or Co²⁺ ions)². ECF-type ABC transporters fall into two groups³. In group I the energizing module is used by a single S-component ('dedicated' energizing modules). The biotin transporter BioMNY from *Rhodobacter capsulatus* is the best-characterized member of this group⁴. In ECF transporters of group II, the same energizing module is shared by several different S-components with different substrate specificities. These S-components are 20–25 kDa in size and predicted to have 4–6 hydrophobic membrane-spanning segments, but they are unrelated at the sequence level, and it is not known whether they are evolutionary related. A crystal structure (at 3.6-Å resolution) is available only for the riboflavin-specific S-component RibU from *Staphylococcus aureus* (PDB 3P5N)⁵.

The group II proteins are particularly abundant in Gram-positive organisms. For example, in *Lactococcus lactis* eight different

S-components interact with the same energizing module⁶, allowing the ECF complexes to transport a wide variety of chemically different substrates. These complexes have a 1:1:1 subunit stoichiometry (S-component:EcfT:EcfA:EcfA'; Fig. 1a), indicating that the S-components are integral parts of the translocating complex, rather than peripherally associated substrate binding proteins⁶. Early *in vivo* transport experiments in *Lactobacillus casei* showed that different S-components dynamically compete for association with the energizing module⁷. The molecular basis for the dynamic interaction between different S-components and the energizing module is unknown.

ThiT is the S-component involved in thiamine (vitamin B₁) transport⁸. It can bind thiamine with very high affinity ($K_d = 120$ pM) and related compounds with nanomolar affinity. High-affinity binding has been observed for other S-components^{9–11} and is most likely important for their biological function. To understand the molecular basis for high-affinity binding and the mechanism of transport by ECF transporters, we determined the high-resolution crystal structure of ThiT from *L. lactis* and present the work in the light of previous and new biochemical data.

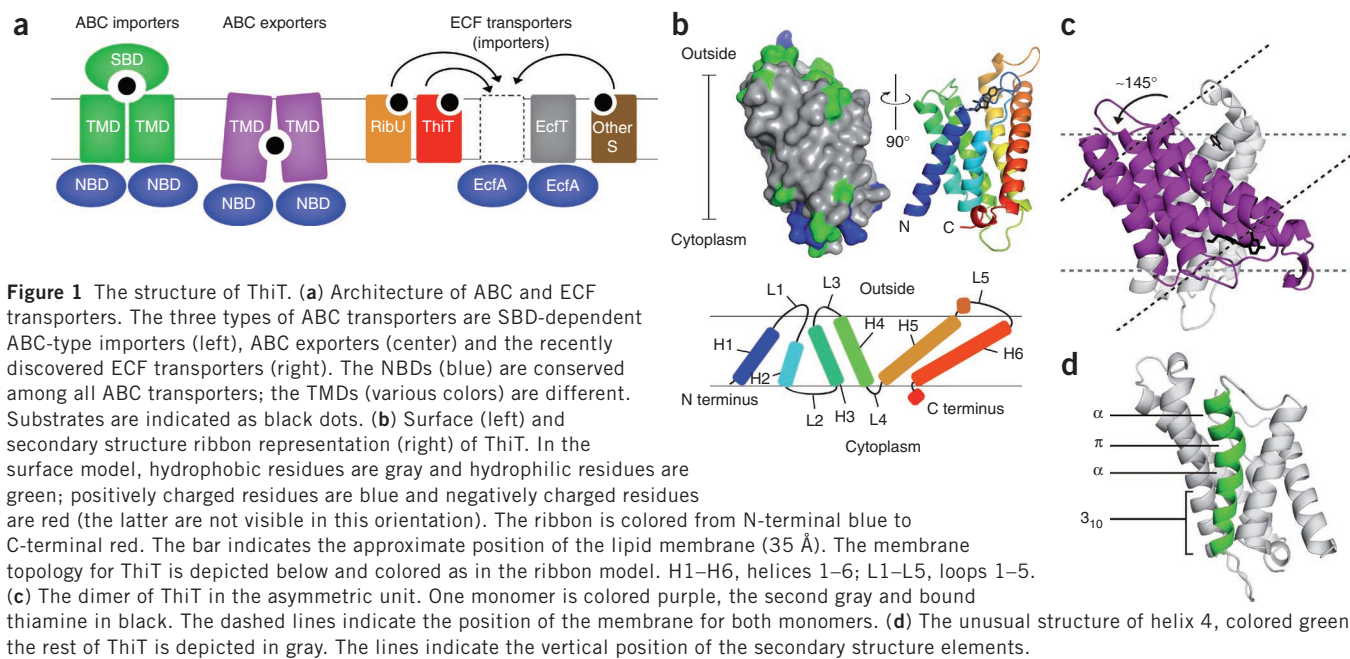
RESULTS

Structure determination of ThiT

We produced ThiT in *L. lactis* NZ9000, which has proven to be a suitable host for membrane protein production with properties complementary to those of *Escherichia coli*¹². The crystal structure of ThiT is the first of a polytopic membrane protein produced in *L. lactis*. We purified ThiT bound to thiamine using the detergent *n*-nonyl- β -D-glucopyranoside. Crystals of the native protein were formed in space group C2 and diffracted to 2.0-Å resolution. We solved the

¹University of Groningen, Groningen Biomolecular Science and Biotechnology Institute, Groningen, The Netherlands. ²University of Groningen, Zernike Institute for Advanced Materials, Groningen, The Netherlands. Correspondence should be addressed to D.J.S. (d.j.slotboom@rug.nl).

Received 12 January; accepted 21 April; published online 26 June 2011; doi:10.1038/nsmb.2073



structure (Fig. 1b and Supplementary Fig. 1) by multi-wavelength anomalous dispersion (MAD) phasing, using crystals of selenomethionine (SeMet)-substituted protein (Table 1). The asymmetric unit contained two copies of ThiT that were virtually identical (r.m.s. deviation = 0.2 Å, Fig. 1c). The entire ThiT sequence could be fitted in the electron

density, with the exception of the N-terminal His tag and the subsequent five or six residues (difference between the two copies of ThiT in the asymmetric unit), which apparently were disordered in the crystals. Almost all residues (98%) were in the preferred regions of the Ramachandran plot, and the remaining 2% were in the additionally allowed regions. The R_{work} and R_{free} values after refinement were 20.4% and 23.2%, respectively. The orientation of the two ThiT molecules in the asymmetric unit is incompatible with the formation of a continuous lipid bilayer, because the membrane plane would have to be rotated $\sim 145^\circ$ at the dimer interface (Fig. 1c), which is highly improbable. Therefore, we believe that the functional unit of ThiT is a monomer in the absence of the energizing module, consistent with previous light-scattering experiments⁸.

Table 1 Data collection, phasing and refinement statistics

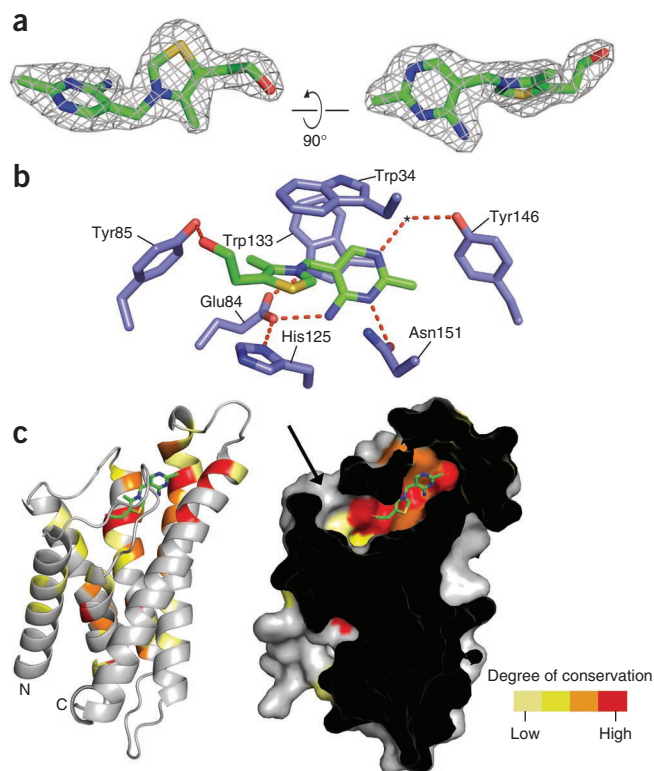
	Native		SeMet-labeled ThiT (Se-MAD)		
Data collection	C2		C2		
Space group	C2		C2		
Cell dimensions					
<i>a</i> , <i>b</i> , <i>c</i> (Å)	61.4, 84.3, 127.0		65.2, 83.7, 128.5		
α , β , γ (°)	90.0, 95.7, 90.0		90.0, 95.9, 90.0		
		Peak	Inflection	Remote	
Resolution (Å)	47.5–2.0	48.9–2.9	48.9–2.9	48.9–2.9	
R_{sym}	6.6 (48.6)	6.9 (27.3)	5.1 (12.7)	4.4 (7.2)	
$I / \sigma I$	8.4 (2.1)	15.7 (6.0)	21.2 (10.2)	26.7 (15.5)	
Completeness (%)	99.0 (96.6)	99.9 (99.9)	99.9 (100)	99.9 (100)	
Redundancy	3.7	6.9	6.9	6.9	
Refinement					
Resolution (Å)	47.5–2.0				
No. reflections	41,123				
$R_{\text{work}} / R_{\text{free}}$	20.4 / 23.2				
No. atoms					
Protein	2,748				
Thiamine	36				
Water	73				
B-factors					
Protein	41				
Thiamine	36				
Water	51				
R.m.s. deviations					
Bond lengths (Å)	0.018				
Bond angles (°)	1.68				

Values in parentheses are for highest-resolution shell.

Well-defined non-protein electron density became visible during refinement that could be assigned unambiguously to thiamine (discussed below). In addition, we found electron density that fitted acyl chains surrounding the hydrophobic parts of the protein. In six cases, there was connected electron density that could fit the headgroup of the detergent *n*-nonyl- β -D-glucopyranoside, and in these cases, we modeled the entire detergent molecule. In the remaining six cases, it was not clear whether the acyl chains belonged to the detergent or to copurified lipids. In these cases, we modeled the acyl chains from the detergent in the electron density.

Overall fold of ThiT and S-components
The overall fold of ThiT from *L. lactis* is similar to that of RibU from *S. aureus* (r.m.s. deviation = 3.5 Å for 145 C α atoms),

Figure 2 The high-affinity thiamine-binding site. (a) Electron density for thiamine shown in gray mesh ($2F_o - F_c$ map contoured at 1.5σ), with the modeled thiamine molecule. (b) Residues forming hydrogen bonds and aromatic interactions with thiamine. Carbon atoms of the thiamine molecule and side chains of the binding residues are shown in green and blue, respectively. Hydrogen bonds are indicated by the red dashes. Tyr146 interacts with thiamine through a water molecule (black asterisk). (c) Ribbon and sliced-surface models of the ThiT structure with the conserved amino acids in ThiT homologs colored according to their conservation score. The arrow indicates the access to the cavity that can accommodate phosphate moieties of TMP and TPP.



although at the sequence level the two proteins are unrelated (14% sequence identity). In the past few years, a growing number of membrane protein structures have been determined that share a related fold without being related in sequence (for example, the LeuT and the aquaporin folds^{13,14}). These observations raise noteworthy questions about the evolution of membrane proteins and the relation between primary and tertiary structures. The lack of sequence conservation between S-components of the ECF transporters is all the more unexpected, because these proteins interact with a common partner, the shared ECF energizing module.

ThiT contains six hydrophobic helical segments that cross the membrane (Fig. 1b). A part of the L1 loop is also embedded in the lipid bilayer, which is necessary because helix 2 is too short to span the entire thickness of the membrane. The position of L1 may play an important mechanistic role in the translocation of thiamine across the membrane (see Discussion). The structure of helix 4 is highly irregular. It starts with the backbone hydrogen-bond pattern of a regular α -helix, then turns into a π -helix¹⁵, returns to an α -helical conformation, and finally continues as a long (seven residues) 3_{10} -helix¹⁶ (Fig. 1d, helix in green). This unusual combination of structural features has not been observed in any other membrane protein structure. For example, in the RibU structure, helix 4 is a regular transmembrane α -helix. The π -bulge irregularity is important for ligand binding and will be discussed in more detail below. The 3_{10} -helical segment allows a very tight packing of transmembrane segment 4 with helices 2 and 3, and—to a lesser extent—helix 5. This close packing is further facilitated by the presence of numerous conserved glycines in helices 3, 4 and 5 and in loop L2 (Supplementary Fig. 2).

Structural basis of high-affinity thiamine binding

The thiamine-binding site is located in a pocket near the extracellular side of the membrane and lined by helices 4, 5 and 6 and the loops L1 and L5. The thiamine molecule was modeled in clear electron density (Fig. 2a) and has a conformation that is different from the catalytic V-shaped conformation observed in enzymes that use thiamine pyrophosphate as a cofactor¹⁷. A large number of interactions shape the binding site and account for the high binding affinity (Fig. 2b and Supplementary Fig. 3). Glu84 in helix 4 stabilizes the positively charged N2 of the thiazole ring, and the adjacent residue Tyr85 forms a hydrogen bond with the hydroxyl group of thiamine. Both residues are located in helix 4, and their favorable orientation is dependent on the π -bulge irregularity in this helix. Hydrogen bonds are formed by Tyr146 (through an ordered water molecule) and Asn151 in helix 6 with the N1 and N3 of the pyrimidine ring, respectively. Trp34 in L1 and His125 (helix 5) are involved in aromatic π -stacking on opposite sides of the thiazole ring, and Trp133 in L5 stacks with the pyrimidine ring. Gly129 allows the pyrimidine ring to pack closely against the C-terminal end of helix 5. The side chains that interact directly with the substrate are held in place by an intricate network of hydrogen bonds and aromatic interactions with other binding residues. In addition, more distant residues that are

not directly involved in substrate coordination contribute to this network (Supplementary Table 1). The structure of the thiamine-binding site is in excellent agreement with previous mutagenesis studies⁸: mutations of Trp133, Gly129, Asn151 and Tyr146 to alanine reduced the binding affinity by a factor of between 20 and 1,000. In contrast, the W34A mutant still bound thiamine with wild-type affinity. Trp34 acts as a lid on the binding site, and its removal apparently has little effect on the rest of the binding site.

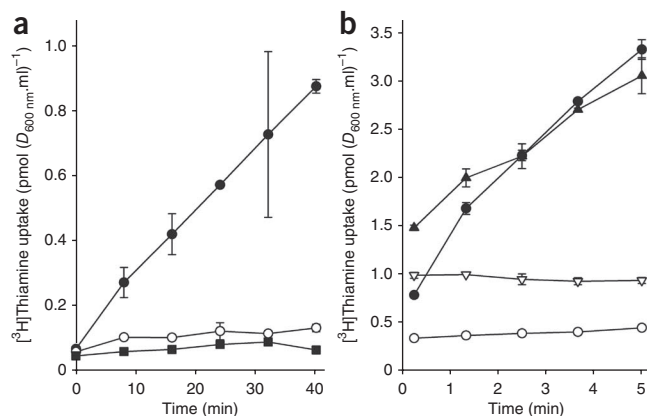
The hydroxyl group of thiamine is accessible from the extracellular environment through a narrow opening expanding into a cavity (Fig. 2c). The cavity does not allow the substrate to enter but provides sufficient space to accommodate the phosphate moieties of thiamine monophosphate and thiamine pyrophosphate (TMP and TPP), which also bind with high affinity to ThiT⁸. Entrance of thiamine into the binding site from the external side of the membrane would require conformational changes of loops L1, L3 and L5, which form a cage of aromatic side chains on top of the substrate.

Substrate transport by ThiT requires the energizing module

The residues involved in thiamine binding are highly conserved among ThiT orthologs (Supplementary Fig. 2). In Figure 2c, the degree of conservation is projected on the ThiT structure. In addition to the binding site residues, a few other amino acids are also strongly conserved (for example, Pro43 at the beginning of helix 2 and several glycines in L2, helix 3 and the 3_{10} part of helix 4). These residues are likely to have a structural role (causing close packing of helices 3 and 4 and capping the short helix 2). We do not observe an obvious translocation path lined with conserved amino acids within ThiT, in contrast to what has been suggested for RibU⁵ (see Discussion). The absence of a translocation path is consistent with thiamine-transport assays (Fig. 3). When expressed in *E. coli*, ThiT alone did not support thiamine transport, but coexpression of the energizing module (EcfAA'T) and ThiT led to robust thiamine uptake. Overexpression of ThiT in *L. lactis* resulted in

Figure 3 Transport of [³H]thiamine in *E. coli* and *L. lactis* cells.

(a) Thiamine uptake by recombinant *E. coli* cells. *E. coli* cells expressing ThiT and EcfAA^T from *L. lactis* (●) or ThiT alone (○), and control cells containing an empty expression plasmid (■), were assayed for thiamine uptake. All cells were energized with glucose. (b) Thiamine uptake by recombinant *L. lactis* cells. De-energized control cells (harboring an empty plasmid but containing chromosomal copies of the genes *thiT* (also known as *llmg_0334*) and *ecfAA^T* (*cbiO*, *cbiQ*, *cbiQ2*) (○), de-energized cells expressing ThiT from a plasmid (▽), energized control cells (●) and energized cells expressing ThiT (▲) were assayed for thiamine uptake. Thiamine binding, rather than transport, was observed in the de-energized cells. The levels of binding depended on the expression levels of ThiT. In the energized cells harboring the empty plasmid, rapid thiamine uptake was observed. In energized cells overexpressing ThiT, the offset on the y axis—indicative of binding—increased, rather than the uptake rate. All experiments were conducted at least in duplicate. The error bars indicate the range (a) or s.d. (b).



increased levels of thiamine binding to the cells but not in increased transport rates. In *L. lactis* the energizing module is constitutively expressed from the chromosomal copy of the *ecfAA^T* genes, and the results show that thiamine transport in *L. lactis* is limited by the amount of EcfAA^T rather than by the amount of ThiT. These experiments, together with previous data⁸, show that ThiT binds thiamine but does not translocate the vitamin in the absence of the energizing module.

Interaction with the EcfT subunit

The lack of sequence similarity between ThiT and RibU is unusual, because both proteins interact with ECF energizing modules, but as the two proteins are from different organisms, they do not interact with the same energizing module. However, ThiT and RibU proteins from the same organism are also unrelated in sequence (for example, in *L. lactis* there is only 16% identity between them). Because of the absence of detectable sequence conservation between the two different S-components, we searched for structural motifs that could be the docking sites for the energizing module. Interaction with the hydrophobic EcfT subunit is expected to take place within the hydrophobic core of the lipid bilayer. A superposition of the ThiT and RibU structures (Fig. 4a)

revealed that helices 1, 2, 3—and to a lesser extent helix 6—align well, but that helices 4 and 5 adopt very different conformations. The structural variability in the latter region is required for correct positioning of the side chains that create the binding sites for either thiamine or riboflavin, and this makes it unlikely that the EcfT component interacts here. In contrast, the surface formed by helices 1, 2, 3 and 6 is very similar in RibU and ThiT. Prompted by this observation, we searched for patterns of sequence conservation in this region that might have been overlooked previously. Sequence comparison of all eight S-components from *L. lactis* revealed that there is a shared alanine motif (AxxxA, where x can be any amino acid) on the exposed face of helix 1 (Fig. 4b, Supplementary Fig. 4). Such tetrad repeats of small amino acids are well known to promote helix-helix interactions between membrane proteins in the lipid bilayer^{18–20}. To test whether the alanine motif was involved in the interaction with EcfT, we separately mutated the two alanines into tryptophan residues and coexpressed the ThiT mutants with the energizing module in *E. coli*. Both mutations (A15W and A19W) lead to a complete loss of transport activity (Fig. 4c), even though the ThiT mutants were expressed to at least the same level as the wild type (Fig. 4c, inset). Notably, the integrity and thiamine-binding capacity of the ThiT

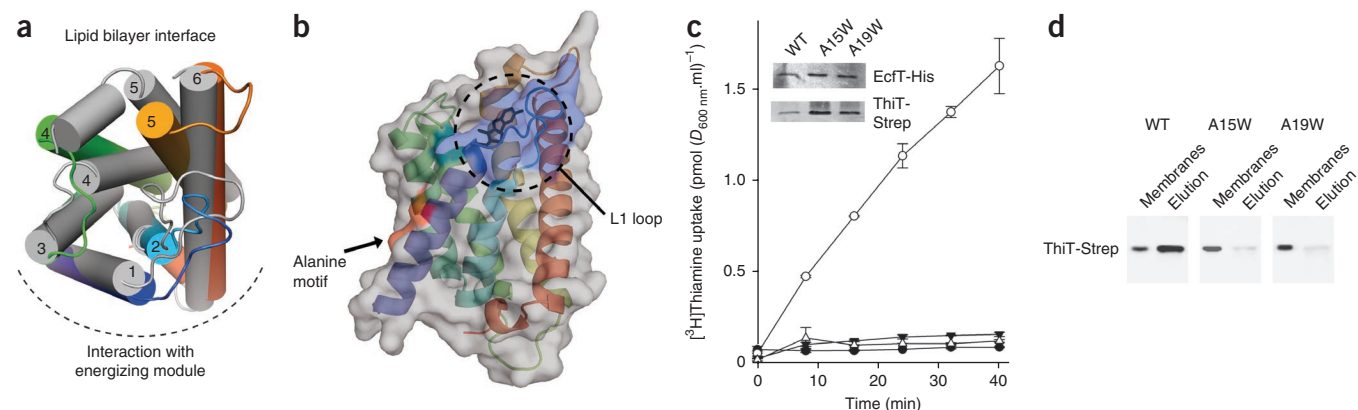


Figure 4 Interaction of ThiT with the energizing module. (a) Superposition of the RibU structure in gray (PDB 3P5N)⁵ on the ThiT structure (colored as in Fig. 1b). The dashed line indicates the proposed interface with the energizing module. The helices are numbered from N terminus to C terminus as in Fig. 1b. (b) The ThiT structure as seen from the interface with the energizing module. The surface of the L1 loop region is highlighted in blue and indicated by the dashed circle. Rearrangement of the L1 loop would expose the bound thiamine (black sticks) to the lateral EcfT interface. The alanine motif in helix 1 that is shared by all S-components in *L. lactis* is colored red. (c) Thiamine uptake by recombinant *E. coli* cells coexpressing EcfAA^T with wild-type ThiT (○), A15W ThiT (△) or A19W ThiT (▼). Thiamine uptake by a control strain harboring an empty plasmid is indicated by the black circles (●). The error bars indicate the upper and lower measured values. The inset shows western blot analyses of the expression levels of His-tagged EcfT (using antibodies directed against the His tag) and Strep-tagged ThiT (using antibodies against the Strep tag). (d) Pull-out experiment. EcfAA^T with a His tag on EcfT was coexpressed with Strep-tagged wild-type ThiT, or variants A15W or A19W in *E. coli* as in c. Membranes were solubilized and the complexes were purified using nickel-affinity chromatography. The elution fractions were analyzed by SDS-PAGE followed by western-blot analysis using antibodies against ThiT-strep.

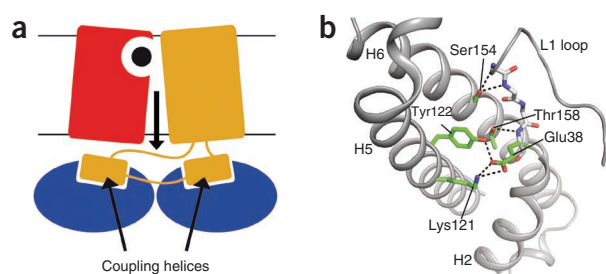


Figure 5 Working model for substrate translocation and interaction with EcfA. **(a)** Model for coupling helix interaction in ECF transporters. The S-component is colored red, EcfT is orange and the EcfA subunits are blue. **(b)** Specific interactions between the L1 loop and helices 5 and 6. Glu38 in L1 forms a salt bridge with Lys121 in helix 5 and a hydrogen bond with Tyr122; the side chains of Ser154 and Thr158 in helix 6 form hydrogen bonds with backbone NH groups in loop L1. In addition, Trp34 in L1 makes an aromatic interaction with Tyr74 in L3 (not shown).

mutants were unaffected by the mutations: the solitary ThiT mutants (in the absence of the energizing module) could be overexpressed and purified in similar amounts as the wild-type ThiT and bound thiamine with high affinity (**Supplementary Fig. 5**). We conclude that the mutations in the alanine motif disrupt the functional interaction between ThiT and the energizing module.

To show that the mutations not only affected the functional interaction between the energizing module and ThiT but also affected complex formation, we conducted a pull-out experiment. We previously showed that the entire complex (EcfAA'T-ThiT) could be pulled out by nickel-affinity chromatography using a His tag on EcfT⁶. Here we show that in contrast to wild-type ThiT, the mutants A15W and A19W were not enriched together with EcfT (**Fig. 4d**), indicating that the interaction between ThiT and the energizing module had indeed been disrupted by the single amino acid substitutions.

DISCUSSION

Interaction with the energizing module

GxxxG and AxxxA motifs are frequently found in membrane proteins and are often involved in helix-helix interactions^{18–20}. The results presented here show that the conserved alanine motif (AxxxA) on the exposed, membrane-embedded face of helix 1 in ThiT mediates the interaction with the EcfT protein. Our observation that a single amino acid substitution (either A15W or A19W) is sufficient to disrupt the functional and physical interaction between ThiT and the energizing module provides a first clue about the mechanism of interaction. It will require mapping the complete interface to gain a full understanding of the forces driving the association in the complex.

Interaction with the nucleotide binding domains

The free energy required for the transport of thiamine comes from the hydrolysis of ATP in the EcfA subunits. In all ABC transporters for which crystal structures are available, each NBD contains a groove that binds to a cytoplasmic segment of the membrane domain. The structural elements in the membrane domains that fit in these grooves are short helical segments named 'coupling helices'. The interaction by means of coupling helices allows ATP hydrolysis to be linked to transport^{21,22}. Because EcfA and EcfA' possess all the sequence motifs that are mechanistically important in NBDs associated with ABC transporters^{22–28} (**Supplementary Fig. 6**), it is reasonable to assume that the two proteins also communicate with the membrane subunits by means of coupling helices, but neither ThiT nor RibU has an obvious coupling helix. To explain this paradox, we propose that the EcfT subunit of the

energizing module may contain two coupling helices. EcfT proteins are predicted to have a long and conserved cytoplasmic loop with two moderately hydrophobic helical segments^{3,29} (**Supplementary Fig. 7**). The size of this cytoplasmic domain (109 amino acids) allows the presence of two rather than one coupling helix for interaction with both EcfA and EcfA' (**Fig. 5a**). The free energy released by ATP hydrolysis is then transferred through the EcfT subunit to the S-components. This hypothesis is supported by mutagenesis studies showing that two conserved motifs (30–40 amino acids apart) in the cytoplasmic loops of different EcfT proteins are important for stabilizing the energizing module–S-component complexes²⁹. The absence of a coupling helix in the S-components might facilitate their exchange from complexes with the shared energizing module. Such a dynamic interaction was already suggested in the 1970s, as a result of *in vivo* transport experiments⁷.

Based on the RibU structure⁵, it has been suggested that clusters of positively charged amino acids in the cytoplasmic loops of ThiT and RibU might mediate the interaction with the EcfA subunit. However, we suspect that the clustering of arginines and lysines in cytoplasmic loops is more likely a manifestation of the 'positive inside rule': membrane proteins are usually enriched for these residues in their cytoplasmic loops, and this bias predicts the membrane topology^{30,31}.

The substrate translocation path

We do not observe an obvious translocation path for thiamine within the ThiT molecule. The substrate binding site is located near the extracellular side of the membrane, and the tight helix packing does not allow a substrate to pass through the interior of the protein. Although the same is true for the RibU structure, some researchers speculate on a transport path for riboflavin through the core of the cylinder-shaped RibU molecule⁵ that would be opened by a conformational change and that is lined with moderately conserved amino acids. In the ThiT structure, we do not see a similar arrangement of conserved residues. Furthermore, a number of amino acids in RibU that were classified as conserved on the basis of a multiple sequence alignment with 12 orthologs are not well conserved when a much larger set of RibU sequences is used, whereas the binding site residues are still conserved.

The absence of an intramolecular translocation path in ThiT is consistent with the lack of thiamine transport activity in the absence of the energizing module (**Fig. 3**). Similarly, for riboflavin transport by RibU from *S. aureus*, the energizing module was required⁵ as well. We hypothesize that instead of using an intramolecular translocation path within the S-components, the substrates are translocated at the interface between the S-component and EcfT, in line with the mechanism that classical ABC transporters use to import substrates¹. Contrary to ThiT and RibU, the biotin-specific S-component BioY from *R. capsulatus* has been proposed to have a homo-oligomeric quaternary structure *in vivo*³² and may facilitate biotin transport in the absence of the energizing module⁵.

Interaction of ThiT with the EcfT subunit on the surface formed by helices 1, 2, 3 and 6 (**Fig. 4a**) immediately suggests a mechanism for substrate transport to the cytoplasm. Rearrangement of the membrane-embedded L1 loop, instigated by ATP binding and hydrolysis in the NBDs, could open a lateral gate for thiamine, facing the EcfT subunit (**Fig. 4b**). Furthermore, the L1 loop interacts intimately with three regions (helices 5 and 6 and L3) that contain substrate-binding residues (**Fig. 5b**). Repositioning of L1 will disrupt these interactions and perturb the binding site, thereby reducing the binding affinity and allowing thiamine to leave.

Symmetry of the membrane domains

All available crystal structures of ABC transporters show structural symmetry between the two transmembrane subunits^{22–28}. The symmetry is

most obvious when the two subunits are identical but is also present in the case of heterodimers, where the folds are related. We were not able to detect sequence similarity between the S-components and EcfT, but we cannot exclude the possibility that these proteins are structurally similar but their sequences have diverged beyond recognition. However, the predicted topology and structural organization of EcfT proteins are different from those of the S-components²⁹. Together with our hypothesis that the EcfT component may contain two coupling helices for interaction with the EcfA subunits, these data suggest that ECF transporters are less likely to be symmetrical than classical ABC transporters.

Conclusion

The high-resolution structural data presented here, together with the RibU structure, provide the first glimpse of the transport mechanism of ECF transporters. Further structural and biochemical studies of the complete complexes will now be necessary for full understanding. ECF transporters are exclusively prokaryotic and numerous human pathogens are dependent on the uptake of ECF substrates for survival^{33,34}. For example, ThiT from the human pathogen *Listeria monocytogenes* has proven to be essential for intracellular replication³⁵. Structural and mechanistic understanding of ECF transporters may enable the development of new antibiotics that target these proteins.

METHODS

Methods and any associated references are available in the online version of the paper at <http://www.nature.com/nsmb/>.

Accession codes. The coordinates of the ThiT structure have been deposited in the Protein Data Bank under accession code 3RLB.

Note: Supplementary information is available on the Nature Structural & Molecular Biology website.

ACKNOWLEDGMENTS

We thank the European Synchrotron Radiation Facility and Swiss Light Source for providing excellent beamline facilities. We thank R. Duurkens for conducting transport experiments, D. Colpa for assistance with the pull-out experiments and A.-M. Thunnissen for critically reading the manuscript. This research was supported by the Netherlands Organization for Scientific Research (NWO) (*Vidi* and ALW Open Programma grants to D.J.S., TOP subsidy grant 700.56.302 to B.P. and Top Talent grant to J.t.B.) and by the European Union European Drug Initiative on Channels and Transporters (EDICT) program.

AUTHOR CONTRIBUTIONS

G.B.E., R.P.-A.B. and D.J.S. designed the experiments. G.B.E., R.P.-A.B., F.F., M.M., A.V.-Z. and J.t.B. conducted the experiments. G.B.E., R.P.-A.B., B.P. and D.J.S. analyzed the data. G.B.E., B.P. and D.J.S. wrote the manuscript.

COMPETING FINANCIAL INTERESTS

The authors declare no competing financial interests.

Published online at <http://www.nature.com/nsmb/>.

Reprints and permissions information is available online at <http://www.nature.com/reprints/index.html>.

- Davidson, A.L., Dassa, E., Orelle, C. & Chen, J. Structure, function, and evolution of bacterial ATP-binding cassette systems. *Microbiol. Mol. Biol. Rev.* **72**, 317–364 (2008).
- Rodionov, D.A. *et al.* A novel class of modular transporters for vitamins in prokaryotes. *J. Bacteriol.* **191**, 42–51 (2009).
- Eitinger, T., Rodionov, D.A., Grote, M. & Schneider, E. Canonical and ECF-type ATP-binding cassette importers in prokaryotes: diversity in modular organization and cellular functions. *FEMS Microbiol. Rev.* **35**, 3–76 (2011).
- Hebbeln, P., Rodionov, D.A., Alfandega, A. & Eitinger, T. Biotin uptake in prokaryotes by solute transporters with an optional ATP-binding cassette-containing module. *Proc. Natl. Acad. Sci. USA* **104**, 2909–2914 (2007).

- Zhang, P., Wang, J. & Shi, Y. Structure and mechanism of the S component of a bacterial ECF transporter. *Nature* **468**, 717–720 (2010).
- ter Beek, J., Duurkens, R.H., Erkens, G.B. & Slotboom, D.J. Quaternary structure and functional unit of energy coupling factor (ECF)-type transporters. *J. Biol. Chem.* **286**, 5471–5475 (2011).
- Henderson, G.B., Zevely, E.M. & Huennekens, F.M. Mechanism of folate transport in *Lactobacillus casei*: evidence for a component shared with the thiamine and biotin transport systems. *J. Bacteriol.* **137**, 1308–1314 (1979).
- Erkens, G.B. & Slotboom, D.J. Biochemical characterization of ThiT from *Lactococcus lactis*: a thiamin transporter with picomolar substrate binding affinity. *Biochemistry* **49**, 3203–3212 (2010).
- Duurkens, R.H., Tol, M.B., Geertsma, E.R., Permentier, H.P. & Slotboom, D.J. Flavin binding to the high affinity riboflavin transporter RibU. *J. Biol. Chem.* **282**, 10380–10386 (2007).
- Eudes, A. *et al.* Identification of genes encoding the folate- and thiamine-binding membrane proteins in Firmicutes. *J. Bacteriol.* **190**, 7591–7594 (2008).
- Henderson, G.B., Kojima, J.M. & Kumar, H.P. Differential interaction of cations with the thiamine and biotin transport proteins of *Lactobacillus casei*. *Biochim. Biophys. Acta* **813**, 201–206 (1985).
- Kunji, E.R., Slotboom, D.J. & Poolman, B. *Lactococcus lactis* as host for overproduction of functional membrane proteins. *Biochim. Biophys. Acta* **1610**, 97–108 (2003).
- Waight, A.B., Love, J. & Wang, D.N. Structure and mechanism of a pentameric formate channel. *Nat. Struct. Mol. Biol.* **17**, 31–37 (2010).
- Theobald, D.L. & Miller, C. Membrane transport proteins: surprises in structural sameness. *Nat. Struct. Mol. Biol.* **17**, 2–3 (2010).
- Cartailler, J.P. & Luecke, H. Structural and functional characterization of π bulges and other short intrahelical deformations. *Structure* **12**, 133–144 (2004).
- Vieira-Pires, R.S. & Morais-Cabral, J.H. 3_{10} helices in channels and other membrane proteins. *J. Gen. Physiol.* **136**, 585–592 (2010).
- Shin, W., Pletcher, J., Blank, G. & Sax, M. Ring stacking interactions between thiamin and planar molecules as seen in the crystal structure of a thiamin picolonate dihydrate complex. *J. Am. Chem. Soc.* **99**, 3491–3499 (1977).
- Lemmon, M.A., Flanagan, J.M., Treutlein, H.R., Zhang, J. & Engelman, D.M. Sequence specificity in the dimerization of transmembrane α -helices. *Biochemistry* **31**, 12719–12725 (1992).
- Russ, W.P. & Engelman, D.M. The GxxxG motif: a framework for transmembrane helix-helix association. *J. Mol. Biol.* **296**, 911–919 (2000).
- Schneider, D., Finger, C., Prodhil, A. & Volkmer, T. From interactions of single transmembrane helices to folding of α -helical membrane proteins: analyzing transmembrane helix-helix interactions in bacteria. *Curr. Protein Pept. Sci.* **8**, 45–61 (2007).
- Hollenstein, K., Dawson, R.J. & Locher, K.P. Structure and mechanism of ABC transporter proteins. *Curr. Opin. Struct. Biol.* **17**, 412–418 (2007).
- Locher, K.P., Lee, A.T. & Rees, D.C. The *E. coli* BtuCD structure: a framework for ABC transporter architecture and mechanism. *Science* **296**, 1091–1098 (2002).
- Aller, S.G. *et al.* Structure of P-glycoprotein reveals a molecular basis for poly-specific drug binding. *Science* **323**, 1718–1722 (2009).
- Hollenstein, K., Frei, D.C. & Locher, K.P. Structure of an ABC transporter in complex with its binding protein. *Nature* **446**, 213–216 (2007).
- Gerber, S., Comellas-Bigler, M., Goetz, B.A. & Locher, K.P. Structural basis of trans-inhibition in a molybdate/tungstate ABC transporter. *Science* **321**, 246–250 (2008).
- Kadaba, N.S., Kaiser, J.T., Johnson, E., Lee, A. & Rees, D.C. The high-affinity *E. coli* methionine ABC transporter: structure and allosteric regulation. *Science* **321**, 250–253 (2008).
- Oldham, M.L., Khare, D., Quijcho, F.A., Davidson, A.L. & Chen, J. Crystal structure of a catalytic intermediate of the maltose transporter. *Nature* **450**, 515–521 (2007).
- Dawson, R.J. & Locher, K.P. Structure of a bacterial multidrug ABC transporter. *Nature* **443**, 180–185 (2006).
- Neubauer, O. *et al.* Two essential arginine residues in the T components of energy-coupling factor transporters. *J. Bacteriol.* **191**, 6482–6488 (2009).
- von Heijne, G. & Gavel, Y. Topogenic signals in integral membrane proteins. *Eur. J. Biochem.* **174**, 671–678 (1988).
- von Heijne, G. Control of topology and mode of assembly of a polytopic membrane protein by positively charged residues. *Nature* **341**, 456–458 (1989).
- Finkenwirth, F. *et al.* Subunit composition of an energy-coupling-factor-type biotin transporter analysed in living bacteria. *Biochem. J.* **431**, 373–380 (2010).
- Glass, J.I. *et al.* Essential genes of a minimal bacterium. *Proc. Natl. Acad. Sci. USA* **103**, 425–430 (2006).
- Thanassi, J.A., Hartman-Neumann, S.L., Dougherty, T.J., Dougherty, B.A. & Pucci, M.J. Identification of 113 conserved essential genes using a high-throughput gene disruption system in *Streptococcus pneumoniae*. *Nucleic Acids Res.* **30**, 3152–3162 (2002).
- Schauer, K., Stolz, J., Scherer, S. & Fuchs, T.M. Both thiamine uptake and biosynthesis of thiamine precursors are required for intracellular replication of *Listeria monocytogenes*. *J. Bacteriol.* **191**, 2218–2227 (2009).

ONLINE METHODS

Protein overexpression. Native ThiT containing an N-terminal His₈ tag (ThiT-nHis) was overexpressed in *L. lactis* strain NZ9000 (ref. 36). The cells were grown semi-anaerobically in GLS medium (2% (w/v) Gistex (Brenntag), 2.5% (w/v) glucose, 100 mM KH₂PO₄, 110 mM K₂HPO₄ and 5 μg ml⁻¹ chloramphenicol). The initial pH was 6.8 and decreased during cell growth. At $D_{600\text{ nm}}$ of 1.5 (at this point the pH was 6.5), expression was induced by the addition of 0.1% (v/v) of culture supernatant from the nisin A-producing strain NZ9700 (ref. 36). The cells were induced for 2 h and reached a final $D_{600\text{ nm}}$ of 4–5. The preparation of membrane vesicles was carried out as previously described⁸. Expression of SeMet (Acros Organics)-substituted ThiT was done in *L. lactis* as previously described³⁷.

Purification of thiamine-bound ThiT-nHis. ThiT-nHis was purified as previously described⁸ with the following modifications: during solubilization, 100 μM thiamine-HCl (Sigma) was added to ensure saturation of all binding sites with thiamine. Membrane vesicles from *L. lactis* NZ9000, expressing ThiT, were solubilized in 1.0% (w/v) *n*-dodecyl-β-D-maltopyranoside (DDM, Anatrace), but in all subsequent steps, this detergent was replaced by 0.35% *n*-nonyl-β-D-glucopyranoside (NG, Anatrace). Size-exclusion chromatography (SEC) was done on a Superdex-200 column (GE Healthcare) in 20 mM HEPES buffer, 150 mM NaCl and 0.35% NG (pH 7.0, adjusted with NaOH). The peak fractions after SEC were concentrated on a Vivaspin 30-kDa molecular weight cutoff (MWCO) concentrator (VWR International) to 6–8 mg ml⁻¹. Concentrated ThiT was used directly to set up crystallization trials.

Crystallization. Initial crystals of ThiT were obtained under several conditions by screening commercially available crystallization conditions with ThiT purified in *n*-octyl-β-D-glucopyranoside (OG, Anatrace), using a dispensing robot (mosquito, TTP Labtech). These crystals were small and diffracted only to ~50 Å. Optimization of the crystallization conditions gradually improved the diffraction properties and finally yielded crystals diffracting to 7–8 Å. Rescreening with the detergent *n*-octyl-β-D-thioglucopyranoside (OTG, Anatrace) resulted in bigger crystals that diffracted up to 5–6 Å. A major improvement was obtained with ThiT purified in NG. Crystals ranging in size from 50 to 300 μm could be grown at 5 °C from a solution containing 15–20% (w/v) PEG 3350 (Hampton Research) and 0.1–0.3 M NH₄NO₃. The crystals appeared within 1 week, grew to full size in 3–4 weeks and diffracted to ~2 Å. For cryoprotection, a solution of 40% (w/v) PEG 3350 was prepared with the same concentration of NH₄NO₃ as for the crystallization condition. Replacing PEG 3350 by PEGs with a higher or lower molecular weight resulted in crystals in most cases, but the best diffraction properties were obtained with PEG 3350. SeMet-substituted ThiT-nHis could be purified and crystallized under conditions identical to those for the native protein.

Structure determination. Diffraction data were collected at the ESRF and SLS beamline facilities. Multi-wavelength Anomalous Dispersion (MAD) data on SeMet-ThiT to 2.9 Å were collected at 100 K on ID29 at ESRF around the K-absorption edge of selenium with wavelengths for remote of 0.9768 Å, for inflection of 0.9793 Å and for peak of 0.9791 Å, in that order. Native data to 2.0 Å were collected at 100 K and 1.0723 Å on ID23-1. Data processing and reduction were carried out using XDS³⁸ and programs from the CCP4 suite³⁹. Relevant statistics for the data collection, phasing and model refinement can be found in **Table 1**. Initial phase information was found and the initial model built using Phenix AutoSol⁴⁰ and Resolve (within Phenix). Four selenium sites were found within the asymmetric unit, corresponding to two SeMet substitutions per protein

molecule (Met17 and Met68). All SeMet peaks were above 25σ (**Supplementary Fig. 8a**). The full model was built in ARP/wARP⁴¹, using the native data. A few cycles of refinement in Refmac5 (ref. 42), including noncrystallographic symmetry with loose restraints, interspersed with manual model building using Coot⁴³, were necessary to complete the model (**Supplementary Fig. 8b**). The final protein model contains residues 7–182 for chain A and 6–182 for chain B; thus, only the initial five or six residues and the His tag are missing. Water molecules were automatically placed in $F_o - F_c$ Fourier difference maps at a 3σ cutoff level and validated to ensure correct coordination geometries, using Coot. All structure figures were prepared with PyMOL (<http://www.pymol.org/>).

Transport of [³H]thiamine in *L. lactis* and *E. coli*. Transport experiments with *L. lactis* cells were conducted as previously described⁸. To de-energize the cells, we added 20 mM *N*-methyl-α-D-glucopyranoside instead of glucose. The cells were grown in chemically defined medium without thiamine. The scarcity of thiamine in the growth medium induces the expression of the chromosomal *thiT* gene. The energizing module (EcfAA'T) was expressed constitutively from the chromosomal copies of the genes.

E. coli MC1061 cells containing plasmids for expression of ThiT alone or both EcfAA'T and ThiT⁶ were grown on LB medium with 100 μg ml⁻¹ ampicillin. At an $D_{600\text{ nm}}$ of ~0.5, expression was induced by adding 10⁻³% (w/v) L-arabinose. After 2 h of induction, the cells were harvested, washed and resuspended in ice-cold buffer (50 mM potassium phosphate, pH 7.5) to a final $D_{600\text{ nm}}$ of 5 and kept on ice. For the transport assays, the cells were energized with 10 mM glucose for 15 min at 30 °C. Subsequently, [³H]thiamine (American Radiolabeled Chemicals) was added to a final concentration of 25 nM, and at the indicated time points, 200-μl samples were taken and mixed with 2 ml stop buffer (ice-cold 50 mM potassium phosphate, pH 7.5). The suspension was rapidly filtered over a BA-85 nitrocellulose filter, which was subsequently washed once with 2 ml stop buffer. Filters were dried for 1 h at 80 °C, and 2 ml of Emulsifier-Scintillator Plus liquid (PerkinElmer) was added. The levels of radioactivity were determined with a PerkinElmer Tri-Carb 2800 TR isotope counter. For time point zero, 200 μl of cell suspension was added to 2 ml stop buffer containing radioactive thiamine, and this mixture was directly filtered.

Purification of EcfAA'T-ThiT. The experiments were conducted as previously described⁶ with wild-type ThiT, ThiT A15W and ThiT A19W coexpressed with the energizing module. The ThiT mutants were prepared using standard cloning techniques.

36. Kuipers, O.P., de Ruyter, P.G.G.A., Kleerebezem, M. & de Vos, W.M. Quorum sensing-controlled gene expression in lactic acid bacteria. *J. Biotechnol.* **64**, 15–21 (1998).
37. Berntsson, R.P. *et al.* Selenomethionine incorporation in proteins expressed in *Lactococcus lactis*. *Protein Sci.* **18**, 1121–1127 (2009).
38. Kabsch, W. Automatic processing of rotation diffraction data from crystals of initially unknown symmetry and cell constants. *J. Appl. Cryst.* **26**, 795–800 (1993).
39. Collaborative Computational Project Number 4. The CCP4 suite: programs for protein crystallography. *Acta Crystallogr. D Biol. Crystallogr.* **50**, 760–763 (1994).
40. Adams, P.D. *et al.* PHENIX: a comprehensive Python-based system for macromolecular structure solution. *Acta Crystallogr. D Biol. Crystallogr.* **66**, 213–221 (2010).
41. Langer, G., Cohen, S.X., Lamzin, V.S. & Perrakis, A. Automated macromolecular model building for X-ray crystallography using ARP/wARP version 7. *Nat. Protoc.* **3**, 1171–1179 (2008).
42. Murshudov, G.N., Vagin, A.A. & Dodson, E.J. Refinement of macromolecular structures by the maximum-likelihood method. *Acta Crystallogr.* **53**, 240–255 (1997).
43. Emsley, P., Lohkamp, B., Scott, W.G. & Cowtan, K. Features and development of Coot. *Acta Crystallogr. D Biol. Crystallogr.* **66**, 486–501 (2010).